

# The monitoring system of the Pierre Auger Observatory: on-line and long-term data quality controls

C. Bleve<sup>1,2</sup>, G. Cataldi<sup>2</sup>, G. Cocciolo<sup>2,3</sup>, M. R. Coluccia<sup>1,2</sup>, P. Creti<sup>2</sup>, S. D'Amico<sup>2,3</sup>, I. De Mitrì<sup>1,2</sup>, G. Marsella<sup>1,2</sup>, D. Martello<sup>1,2</sup>, L. Perrone<sup>1,2</sup>, V. Scherini<sup>1,2</sup> and the Pierre Auger Collaboration

<sup>1</sup> Dipartimento di Matematica e Fisica “Ennio De Giorgi”, Università del Salento, Italy

<sup>2</sup> Istituto Nazionale di Fisica Nucleare sez. di Lecce, Italy

<sup>3</sup> Dipartimento di Ingegneria dell'Innovazione Università del Salento, Italy

## 1. Abstract

The Pierre Auger Observatory consists of a surface array of 1660 water Cherenkov detectors (SD), overlooked by 27 air fluorescence telescopes (FD) grouped in four sites. A system to monitor the status and the performance of the whole Observatory has been developed to ensure its smooth operation and optimal data quality for physics analysis. In addition to the on-line calculation of the SD exposure and the FD on-time, the available information is used to check the long term stability of key quantities and of data quality, thus defining the performance metrics [ 1].

## 2. Introduction

Designed as a hybrid detector, the Pierre Auger Observatory [ 2], located in Argentina (Pampa Amarilla, 1400 m a.s.l.), uses two techniques to measure the extensive air shower (EAS) properties by observing both their longitudinal development in the atmosphere and their lateral spread at ground level. Charged particles and photons that reach the ground are sampled with the Surface Detector array (SD) which consists of 1660 independent water-Cherenkov detectors (WCDs), filled with 12 tons of pure water each, and equipped with three photomultipliers (PMTs) to detect the Cherenkov light emitted in the water [ 3]. The WCDs are spread on a triangular grid of 1.5 km spacing over 3000 km<sup>2</sup>. The fluorescence light generated in the atmosphere by the charged particles of the air shower through excitation of N<sub>2</sub> molecules is detected by the Fluorescence Detector (FD) [ 4] which consists of 27 telescopes, in five different buildings. The field of view of each telescope is 30° in azimuth, and 1.5° to 30° in elevation, except for three of them, for which the elevation is between 30° and 60° (HEAT telescopes [ 5]). Light is focused with a spherical mirror of 13 m<sup>2</sup> on a camera of 440 hexagonal

photomultipliers. The FD can only operate during dark nights, which limits its duty cycle to 13% while the SD operates 24 hours per day. Stable data taking with the SD started in January 2004 and the Observatory has been running with its full configuration since 2008.

The operation of the whole Observatory is continuously monitored: information on each detector status, as well as on atmospheric devices, are treated to insure its optimised functioning.

## 3. Monitoring system

The basis of the monitoring system is a database running at the central campus. The front-end is web based using common technologies like PHP, CSS and JavaScript. The replication of the databases and the web site is continuously performed to have a mirror site in Europe. Thanks to this, any Pierre Auger researcher can access the present running conditions as well as the performance of the Observatory from their home institute. On the web site, the main page gives an overview of the general features of the running conditions; any trouble is underlined. Dedicated sections exist for each main part of the Observatory, such as the Central Data Acquisition System (CDAS), the SD, the FD, the communication system, the atmospheric monitoring devices, and the status of the monitoring server itself. In the following the functionalities related to the performance of both the SD and FD are described.

## 4. SD and FD on-line monitoring

Since the SD and the FD are operated differently, the monitoring of their status have different requirements.

### 4.1. SD on-line monitoring

The detectors of the surface array operate constantly in a semi-automated mode. The failures

of any WCD component must be detected, and the trigger rates should be controlled. The main page of the SD section displays a summary of the SD array status, where one can have a quick look at trigger rates, at WCDs not sending data (“black tanks”) and at malfunctioning ones, noticed via a list of alarms raised by daily checking processes. Several dedicated pages with links between each other allow the user to display more specific information. In particular one can access the slow control data registered every 400 seconds for each of the 1660 WCDs, such as voltages and currents of the solar power system, photomultipliers and CPU board voltages, environmental parameters as well as calibration data and individual trigger rates.

The trigger for the surface detector array is hierarchical [ 6]. Two levels of trigger (named T1 and T2) are formed at each WCD. The T2 triggers are normally sent to the CDAS; they are combined with those from other detectors and examined for spatial and temporal correlations, leading to an array trigger (T3). The T3 trigger initiates data acquisition and storage. Tables, graphics and maps are available to control T2 triggers, from a page which is regularly refreshed, to get the most up-to-date information for displaying the T2 status and its stability over a short period.

The physics trigger, T4, is designed to select real showers from the set of stored T3 data. The high quality SD trigger level is a fiducial trigger to select only events well contained in the array, ensuring the shower core to be properly reconstructed. It requires that six active detectors surround the detector with the highest signal at the time of shower impact, the seven WCDs forming then an active hexagon.

For this trigger the SD is fully efficient for the detection of EAS with energy above  $3 \times 10^{18}$  eV and zenith angle below  $60^\circ$  [ 6]. In this range of energies and angles, the SD exposure can be determined on the basis of the geometrical aperture. Due to maintenance operation and “black tanks”, the aperture does not reach its nominal value. The number of active hexagons is thus continuously monitored and stored in the database. A dedicated web page of the SD section provides these numbers and a corresponding array map (Fig. 1).

#### 4.2. FD on-line monitoring

The data acquisition for the FD telescopes is organised building-wise to ensure against disruption of data collection due to possible communication losses between the CDAS and the remote

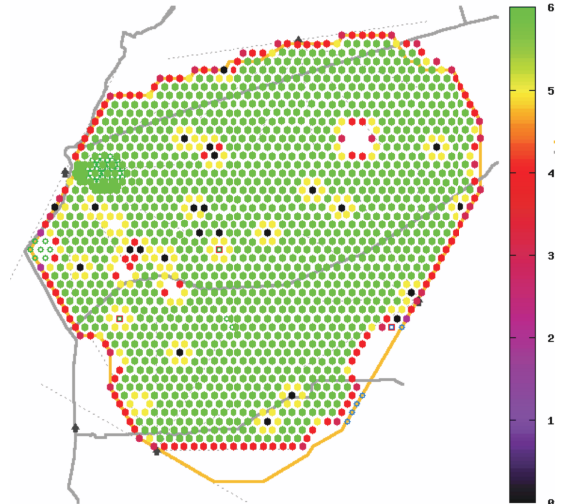


Figure 1. Map of the SD array with the current active detectors (colored points). For each working detector, the color indicates the number of surrounding active detectors.

detectors. For the FD monitoring the data transport is organised via the database internal replication mechanism. This mechanism recognises communication problems and tries to catch up with the submitted database changes when the connection is reestablished, thus guaranteeing completeness of the data-set on the central server.

The data taking of the FD can only take place under specific environmental conditions and is organised in night shifts. The telescopes are not operated when the weather conditions are dangerous (high wind speed, rain, snow, etc.) and when the observed sky brightness (caused mainly by scattered moonlight) is too high. As a consequence, the shifters have to continuously monitor the atmospheric and environmental conditions [ 7] and judge the operation-mode on the basis of the available information.

Alarms, occurrences of states that require immediate action, are first filled into a specified table of the database. The web front-end checks this table for new entries and indicates them on the web page. The shifter is expected to notice and acknowledge the alarm, which then can be declared as resolved once the raised issue is solved.

The information collected for the supervision of the FD operation is split into five sections, dedicated respectively to: i) information from the different levels of calibration (Fig. 2), ii) the background data obtained from each 30 second read-out of the full camera, iii) the DAQ and trigger showing the frequency of fired triggers that

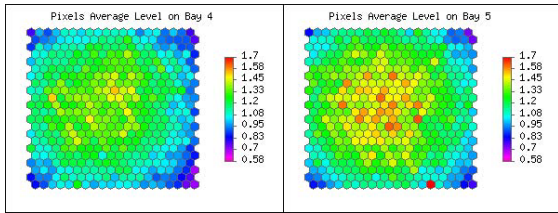


Figure 2. Picture from the web-interface showing a selection of FD-calibration data for two of the six cameras in FD-building Coihueco in a dedicated view representing the PMT arrangement.

indicate the status of the telescopes at an advanced stage, iv) the weather conditions and temperatures, and v) the LIDAR monitoring the atmospheric conditions [ 8] close to the building which is vital for the operation of the telescopes.

## 5. Long-term data quality

### 5.1. Surface Detector

Relevant data useful for long-term studies and for quality checks are stored in the Auger Monitoring database on a one-day basis. Dedicated pages in its SD section web site allow the user to display the evolution with time of the response and of the trigger rates of each Cherenkov detector but also the SD array working status and the quality of the SD data.

Mean values over one day of the number of active SD detectors, of the “black tanks”, the number of active hexagons as well as the nominal one (expected value if all the detectors deployed were active), are stored with other metrics in a dedicated table that can be accessed via the web site. From these information, one can check the evolution of the number of active WCDs and of the active hexagons compared to the existing ones. As an example are shown on Fig. 3 the number of active WCDs normalised to the nominal number of WCDs in the array (left) and the number of active hexagons (right) for the last 3 years.

Each WCD has three PMTs, which are balanced such that they produce on average the same output signal. Due to some identified failures, a small percentage of PMTs should not be considered in the analysis. Each PMT has to fulfill several quality criteria to be used in the analysis. Criteria are based on mean values and standard deviations of the PMT baselines, and on parameters used in the WCD calibration [ 9]. The implementation of the quality cuts is done on a day-by-day basis to provide for each day a list of PMTs showing troubles, stored in a database.

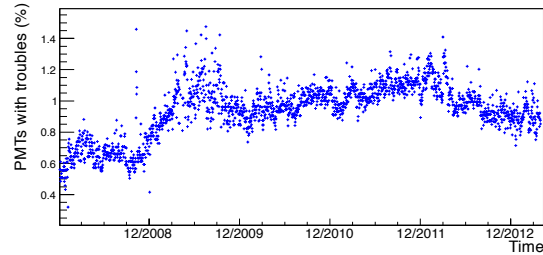


Figure 4. Percentage of PMTs which do not verify the quality criteria among the functioning ones, as a function of time.

The results of the implementation of the quality cut procedure are available via a dedicated SD section. In Fig. 4 we show the percentage of PMTs which do not verify the quality criteria among the functioning ones, since the completion of the array, and this allows us to check the time evolution of the number of rejected PMTs.

The most important parameters of the SD calibration [ 9] are the peak current measured for a vertical muon,  $I_{VEM}^1$  (so-called *peak*) and the corresponding charge  $Q_{VEM}$  (so-called *area*). The calibration procedure allows the conversion of one VEM in electronics units.  $I_{VEM}$  and  $Q_{VEM}$  are available from the local station software using the signal produced by the atmospheric muons. To control the uniformity of the detector response, as well as its evolution with time, the distributions of both the *peak* and the *area* can be displayed for all the PMTs of the SD array. Examples of such distributions are shown in Fig. 5, corresponding to one month of data for two different years. The uniformity and the stability of the calibration parameters ensure a stable and uniform response to shower signals. The decrease of the *area* mean value is due to a convolution of water transparency, Tyvek<sup>®</sup> reflection and electronic response of the WCDs. This does not affect the quality of the data [ 10].

Beside individual trigger rates and PMT parameters of each WCD, which can be checked over long periods, the T3 trigger rates are also monitored since they reflect the evolution of the SD response. As an example, the T3 trigger rate over past year is shown on Fig. 6.

### 5.2. Fluorescence Detector

The calculation of the on-time for each FD telescope is derived by taking into account the status of the data acquisition, of the telescopes, the

<sup>1</sup>VEM: Vertical Equivalent Muon.

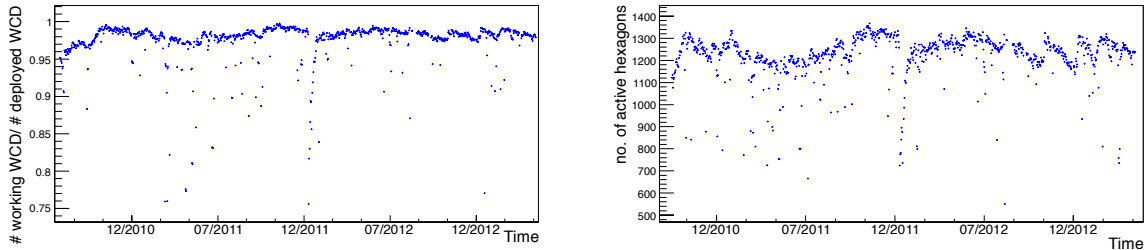


Figure 3. Left: number of active WCDs normalised to the nominal number of WCDs in the array, as a function of time. Right: number of active hexagons as a function of time.

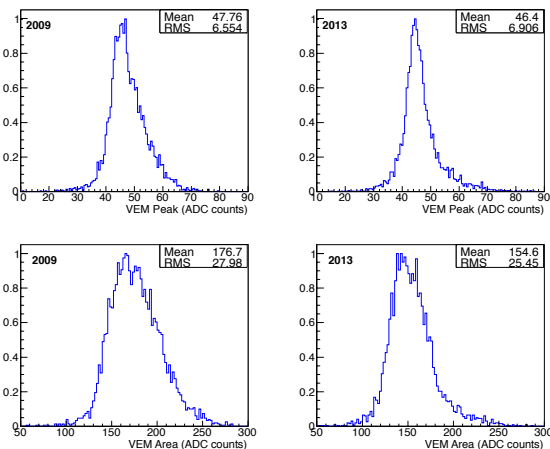


Figure 5. Distribution of the *peak* (top) and *area* (bottom) over all working PMTs (one month of data) for 2 different years.

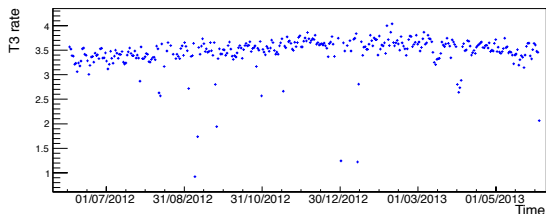


Figure 6. T3 trigger rate over past year.

camera pixels, the communication system, among others. Details of the on-time and exposure calculations, necessary ingredients for the measurement of the energy spectrum, are given in [ 11]. Since July 2007 a tool based on the monitoring system [ 12] is available for the on-time calculation, accounting also for vetoed time intervals

induced by the operation of the LIDAR system or in the case of an excessive rate of FD triggers. The average variances and the on-time-fraction of individual telescopes are calculated for time-intervals of ten minutes, balancing the statistical precision of the calculated on-time with the information frequency. After the initial phase due to the start-up of the running operations the mean on-time is about 13% for all the FD-sites. A program performing the calculation is running on the database server and the appropriate tables are continuously filled in. The web-interface displays the stored quantities. The FD and hybrid<sup>2</sup> on-time of each telescope as well as the accumulated on-time since 1 Jul 2007 for the six telescopes of Coihueco and for the three telescopes of HEAT are plotted on Fig. 7. Similar plots are available for the FD on the monitoring web pages, showing the on-time in quasi real-time for the shifter as a diagnostic and figure of merit.

### 5.3. Hybrid data quality

Thanks to the smooth running of the Observatory, the performance of the hybrid detector is demonstrated as a function of time using a sample of events fulfilling basic reconstruction requirements, such as a reliable geometrical reconstruction and accurate longitudinal profile and energy measurement.

In Fig. 8, the mean energy of the hybrid events above  $10^{18}$  eV with distance to the shower maximum between 7 and 25 km (corresponding to the 90% of the entire hybrid data sample) is shown as a function of time. This plot demonstrates the hybrid data and directly assesses their long term stability.

## 6. Conclusions

The Auger Monitoring system is used to control on-line the running of the Observatory and

<sup>2</sup>Hybrid events are events measured by both FD and SD.

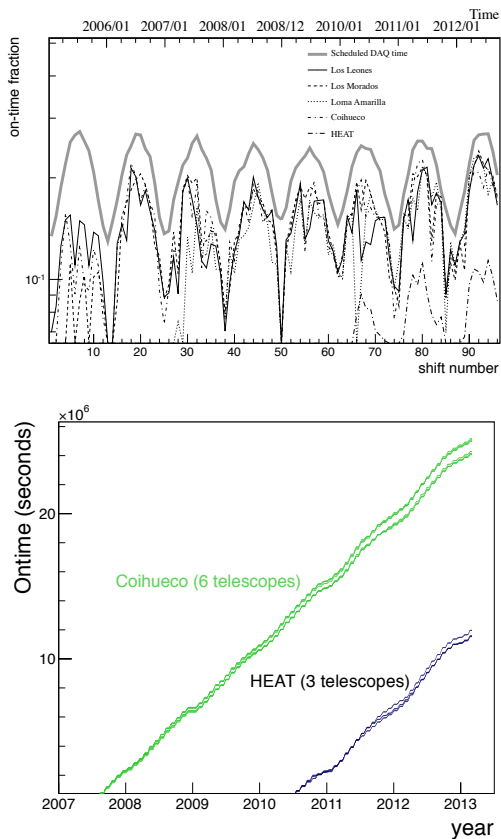


Figure 7. Top: time evolution of the average hybrid on-time fraction for the four FD sites and HEAT. The thick gray line defines the scheduled data-taking time fraction limited to the nights with moon-fraction lower than 60%. Bottom: the accumulated on-time since 1 Jul 2007 for the six telescopes of Coihueco and for the three telescopes of HEAT.

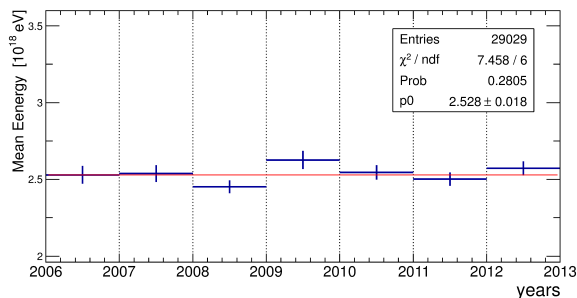


Figure 8. Mean energy for reconstructed hybrid events.

to solve the troubles raised by the alarms. Moreover, it provides also a large number of valuable displays to check the quality of data taking and the long term performances of both the SD and FD.

## REFERENCES

1. C. Bonifazi, for the Pierre Auger Collaboration, Proc. 33rd ICRC, Rio de Janeiro, Brazil, (2013); arXiv:1307.5059
2. The Pierre Auger Collaboration, Nucl. Instrum. Meth. A **523** (2004) 50.
3. I. Allekotte et al, for the Pierre Auger Collaboration, Nucl. Instrum. Meth. A **586** (2008) 409.
4. The Pierre Auger Collaboration, Nucl. Instrum. Meth. A **620** (2010) 227.
5. T. Hermann-Josef Mathes, for the Pierre Auger Collaboration, Proc. 32nd ICRC, Beijing, China **3** 149 (2011); arXiv:1107.4807.
6. The Pierre Auger Collaboration, Nucl. Instrum. Meth. A **613** (2010) 29.
7. The Pierre Auger Collaboration, JINST, **8** P04009 (2013); L. Valore, for the Pierre Auger Collaboration, Proc. 33rd ICRC, Rio de Janeiro, Brazil, (2013); arXiv:1307.5059
8. The Pierre Auger Collaboration, J. Instrum. **7** (2012) P09001.
9. X. Bertou et al, Nucl. Instrum. Meth. A **568** (2006) 839.
10. R. Sato, for the Pierre Auger Collaboration, Proc. 32nd ICRC, Beijing, China **3** (2011) 200; arXiv:1107.4806.
11. The Pierre Auger Collaboration, Astropart. Phys. **34** (2011) 368.
12. J. Rautenberg, for the Pierre Auger Collaboration, Proc. 31st ICRC, Lodz, Poland (2009); arXiv:0906.2358.